A MULTI-MODULE CAVITY STRUCTURE OF SPLIT COAXIAL RFQ

E. Tojyo, S. Arai, T. Fujino, T. Fukushima, N. Tokuda
Institute for Nuclear Study, University of Tokyo,
Tanashi-shi, Tokyo 188, Japan

T. Hattori
Tokyo Institute of Technology,
Ohokayama, Meguro-ku, Tokyo 152, Japan

Abstract

In the development of a split coaxial RFQ with modulated vanes, a multi-module cavity structure has been used to achieve the easy alignment of vanes and the mechanical stability of structure. The rf characteristics of the structure such as the effects of the stems and electrode shape on the resonant frequency are examined by using a 1/4 scaled model with flat vanes. The results of experiments are compared with calculations. The proton acceleration test is in preparation, where the 1/4 scaled model is used by replacing the flat vanes by the modulated vanes.

Introduction

A multi-module cavity structure of split coaxial RFQ[1,2] has been developed based on the new idea to support the vanes by stems at several points for improving the vane alignment and mechanical stability. This structure is different from the split coaxial RFQ of single cavity [3,4,5] and has some unknown rf characteristics with respect to the mode separation, the field distribution, the reduction of quality factor and so on. Then, a 1/4 scaled model of a uranium machine with flat vanes has been fabricated and the mechanical properties and rf characteristics have been examined.

This model consists of 4-module cavities and the dimensions of each module are 40 cm in diameter, 50 cm in length and 7.5 cm in stem width. In order to accomplish the vane positioning, the parts for positioning have been manufactured with accuracy better than ±0.025mm. The 4-module tanks are aligned on a basis like a V-bett machined with accuracy within ±0.025mm. The vane positioning has been achieved with accuracy within ±0.1mm[6].

As for the rf characteristics, before the experimental study, it was concerned whether the stable resonant mode is obtained and whether both end modules affect the field flatness. However, it was confirmed experimentally, there are not such problems as mentioned above. On the other hand, it has been clarified that the effect of stems on the resonant frequency is fairly strong and the cross-sectional shape of inner conductor affects also the resonant frequency. Then, in order to examine the effect of stems, we have measured rf characteristics systematically by closing the both ends of each module with end-plates.

The effect of cross-sectional shape of inner conductor on the inductance of the cavity has been examined by installing the various inner conductors in a small split coaxial cavity made of aluminium. The experimental results with respect to these problems are reported in the present paper.

As the next step of the development, proton acceleration is in preparation. For the acceleration test, the flat vanes in the 1/4 scaled model is replaced by the modulated vanes. The outline of this project is also reported.

RF Characteristics

Effect of Stems

In order to examine the effect of stems on the resonant frequency and field distribution, rf characteristics have been measured on the 1/4 scaled models with and without end-plates in each module. By comparing the difference of experimental results between two cases, following effects of stems have been clarified.

1) The resonant frequencies of the fundamental and higher harmonics modes at the structure with end-plates are generally higher than without end-plates as shown in Table 1. This result shows that the stems between adjacent modules increase the inductance of structure. Therefore, inductance due to the stems should be taken into account in addition to the coaxial like inductance.

Table 1. Resonant frequencies of structure with and without end-plates.

No. of harmonics	With end-plates	Without end-plates
1	37.1200 MHz	41.7616 MHz
2	75.0892	76.2687
3	132.994	132.879
4	185.362	187.968

2) In the case of 4-module cavity structure, the number of end-plates set inside the structure are 3 in all. Every time when an end-plate is mounted, the resonant frequency of the fundamental mode has been measured. The change of resonant frequency due to the end-plates is shown in Fig.1. This resonant frequency change is explained well by the calculation where the stem inductance is considered.

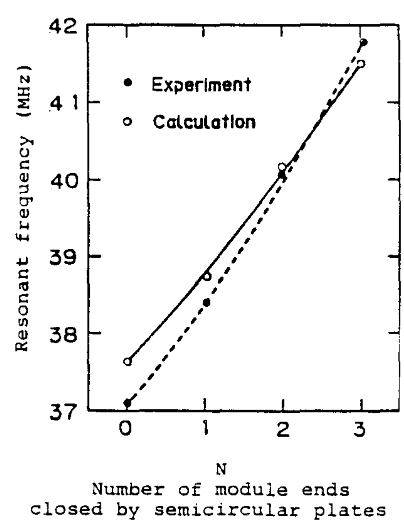

N	Resonant frequency (MHz) ○	●
0	37.7	37.11
1	38.8	38.40
2	40.2	40.09
3	41.5	41.76

Fig. 1. Relation between the resonant frequency and the number of end-plates installed in the four-module cavity structure.

3) Un loaded Q-value of the structure with three end-plates is about 20% higher than one without end-plate.

4) The flatness of the longitudinal electric field distribution is within ±2.5 even if the end-plates are

used or not.

Results of the calculation and the experiment are summarized in Table 2. From these results, following matters are discussed. When the end-plates are installed in all modules, the resonant frequency and the unloaded Q value become higher than when the end-plate is not installed. On the other hand, the flatness of longitudinal field distribution is not different in both cases. Therefore, these features on rf characteristics should be taken into account as well as the mechanical features, when the multi-module cavity structure is employed.

Table 2. Comparison between calculations and experiments on a 1/4 scaled model.

	Without end-plates		With end-plates		Unit
	Calculation	Measurement	Calculation	Measurement	
Inductance	48.4	49.8	159.5	157.1	nH
Resonant frequency	37.7	37.1	41.5	41.8	MHz
Resonant resistance	120	80	135		kΩ/module
Unloaded Q	2650	2000	3250	2320	

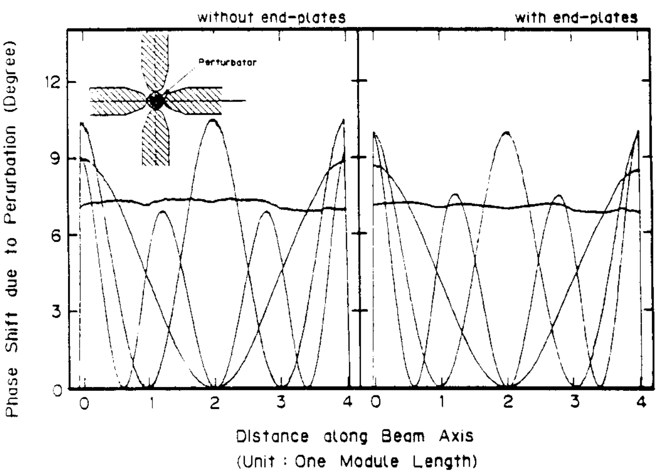

Fig. 2. Longitudinal field distributions of the fundamental and higher harmonics modes; left and right show the cases without and with end-plates.

Effect of Electrode Shape

It has been found out in the rf measurement on a 1/4 scaled model that the cross-sectional shape of inner conductor affects the inductance of cavity remarkably. A small split coaxial cavity of aluminium has been made for examining the relation between electrode shape and resonant parameters. Its dimensions are 134mm in inner diameter and 280mm in length. Four kinds of electrode shapes have been made as split electrode. Resonant frequency and static capacitance have been measured for each electrode shape.

On the other hand, by using the estimated value of inductance and the measured value of static capacitance for each shape, the resonant frequency has been calculated for each shape. The calculated frequency is compared with measured one in Table 3. In order to estimate the inductance of cavity, two methods are used. At the first method, it has been assumed, that the current of inner conductor concentrates on the outer surface of the beam of each electrode, and magnetic flux between the inner conductor and the outer conductor has been calculated numerically.

The difference between the estimated frequency and the measured one is within 2-4%. The result estimated by the same method on the 1/4 scaled model is compared also with experimental one in Table 2.

Table 3. Comparison between calculations and experiments on a small split coaxial cavity with various electrode shapes.

Shapes of Electrodes	Measured Static Capacitance C (pF)	Inductance (nH)			Resonant Frequency (MHz)		
		L_1	L_2	L_3	Measured fom	Calculated foc	fom / foc
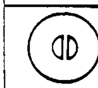	84.0 spaced with acryl plates	63.38	61.1		68.97	70.25	0.98
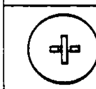	82.4	64.38	55.2	69.1	69.10	74.62 66.72	0.93 1.04
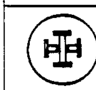	89.2	50.75	45.1	51.8	74.79	81.10 74.00	0.92 1.01
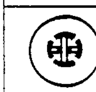	99.5	51.31	48.6		70.43	72.71	0.97

$L_1 = \frac{1}{(2\pi f_{om})^2 C}$: Calulated from measured value.

$L_2 = \frac{\mu_0 l}{2\pi} \ln \frac{r_b}{r_a}$: Calculated by coaxial line approximation.

$L_3 = \frac{\int B ds}{I}$: Calculated by magnetic field integral.

At the second method, the inductance of cavity has been approximated by the inductance of coaxial line, that is, the inner conductor has been assumed to be cylindrical. The calculated values of resonant frequency are about 2-8 % different from measured values. This method is not suitable for estimation of the resonant frequency at the electrode shape used in the 1/4 scaled model.

The penetration of the azimuthal magnetic field into the space between adjacent vanes has been examined at the electrode with rectangular plate beam which is similar to one of the 1/4 scaled model. In this experiment, variation of the cavity inductance has been measured by perturbation method at the points of 16 in a quardrant space of the inner conducter. The measurement method is as follows: a metal rod is set parallel to the axis in each point and the capacitance and the resonant frequency are measured. By using these two quantities, the inductance of the cavity has been measured systematicaly. The difference of inductance between the rod-filled state and the empty state is plotted at each point in Fig.3.

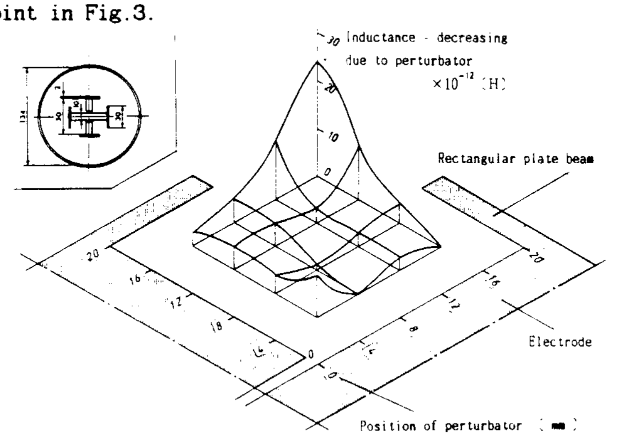

Fig. 3. Change of the inductance measured by a perturbation method.

Preparation for the Proton Acceleration Test

Based on the remarkable achievements on the 1/4 scaled model with flat vanes, a model of uranium RFQ 'AMOUR' has been designed to accelerate proton beam. Figure 4 shows a test stand for the proton acceleration where an ion source of a compact ECR type is used. The purpose of construction of accelerating model is to evaluate synthetically the performance of a vane type split coaxial RFQ which adoptes a multi-module cavity structure. In the vane design, this model can accelerate the ions with charge to mass ratio of 1/15 from 2 keV to 60 keV. In fact, proton acceleration is enough to examine the problems on the beam dynamics.

Beam dynamics parameters are summarized in Table 4. As for vanes, the copy of TALL vanes [7] will be used by the economical reason. TALL is operated at 100 MHz. Therefore, the characteristics of the beam dynamics has been investigated when the TALL vanes have been operated at a frequency of 50 MHz.

Table 4. Design parameters of a model of uranium RFQ.

	Design	
Charge to mass ratio	0.06667	
Frequency (f)	50	MHz
Kinetic energy (T)	2.00 – 59.6	keV/u
Normalized emittance (ε_N)	0.03	π cm·mrad
Kilpatrick factor	1.23	
Intervane voltage (V)	43.5	kV
Focusing strength (B)	3.8	
Max. defocusing strength (Δ_b)	-0.075	
Synchronous phase (ϕ_s)	-90 – -30	deg
Max. modulation (m_{max})	2.48	
Number of cells	168	
Vane length	205.19	cm
Mean bore radius (r_o)	0.541	cm
Min. bore radius (a_{min})	0.294	cm
Margin of bore radius (a_{min}/a_{beam})	1.15	
Transmission (0 emA)	84	%
(2 emA)	69	%
(4 emA)	56	%

The problem interested in the beam dynamics is how a potential on the beam axis affects the transmmision efficiency and the divergence of output beam. For the length of radial matching section, it is necessary to be even times a unit cell length. As shown in Fig.5, variation of the transmission has been calculated as a function of the number of unit cell length by using PARMTEQ.

The variation of transmission due to space charge is shown in Fig.6.

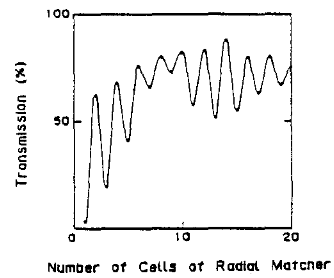

Fig.5

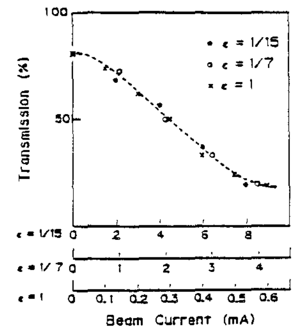

Fig.6

Fig.5. The relation between the transmission efficiency and the length of radial matching section.

Fig.6 The variation of transmission due to space charge.

Conclusion

From the above experimental study, electrical characteristics of the multi-module cavity structure has been clarified. An estimation method for the structure design has been established in the explanation of the experimental results of a 1/4 scaled model and a small alminium model. In the beam simulation for a model of uranium RFQ, it has been clarified that the vanes designed at 100 MHz can be used as vanes operated at 50 MHz.

Acknowledgments

The authors express their sincere gratitude to Professor Y. Hirao for his encouragement. The 1/4 scaled model is manufactured at the machine shop of INS. The beam simulation and structure design have been carried out with the computer FACOM M380 of the INS computer facility.

References

1. S. Arai, GSI-Report 83-11, 1983.
2. S. Arai *et al.*, IEEE Trans. Nucl. Sci., Vol. NS-32, No. 5, October 1985, p. 3175.
3. R. W. Mueller *et al.*, Proc. 1984 Linear Acc. Conf., Seeheim, Fed. Rep. of Germany, p. 77.
4. H. Klein *et al.*, GSI-Report 82-8, 1982, p. 150.
5. A. Moretti *et al.*, Proc. 1981 Linear Acc. Conf., Santa Fe, NM, USA, p. 197.
6. T. Fujino *et al.*, INS-NUMA-59, 1985.
7. N. Ueda *et al.*, IEEE Trans. Nucl. Sci., Vol. NS-30, No. 4, August 1983, p. 2975.

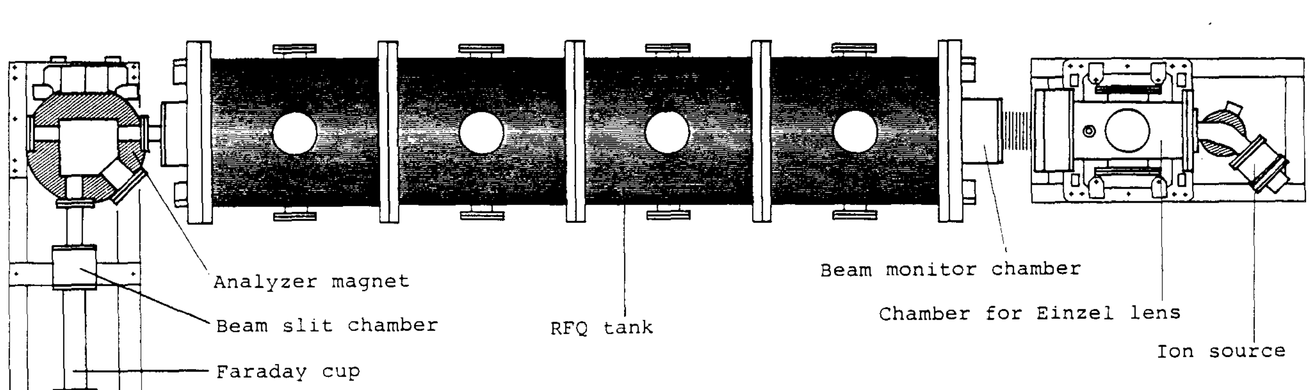

Fig.4 Layout of "AMOUR" test stand